

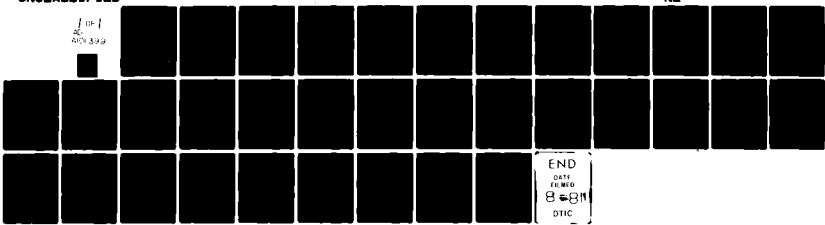
AD-A101 399

SOIL CONSERVATION SERVICE OXFORD MS SEDIMENTATION LAB F/G 20/4  
STREAM CHANNEL STABILITY, APPENDIX N, ALLUVIAL CHANNEL FLOW RES--ETC(U)  
APR 81 N L COLEMAN R B WILSON

UNCLASSIFIED

NL

{ OF }  
AC  
AD-101 399



END  
DATE  
ECHOED  
8-6-81  
DTIC

*f*  
DRAFT FILE COPY

AD A101399

LEVEL  
~~XXX~~

(1)

## STREAM CHANNEL STABILITY

### APPENDIX N

### ALLUVIAL CHANNEL FLOW RESISTANCE: STOCHASTIC PROPERTIES

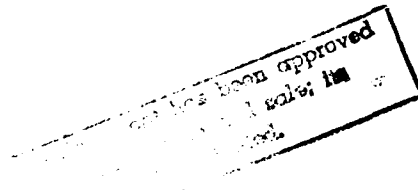
*Project Objective 4*

*by*

*N. L. Coleman and R. B. Wilson*

*USDA Sedimentation Laboratory  
Oxford, Mississippi*

*April 1981*



*Prepared for  
US Army Corps of Engineers, Vicksburg District  
Vicksburg, Mississippi*

*Under  
Section 32 Program, Work Unit 7*



81 7 14 093

STREAM CHANNEL STABILITY•  
APPENDIX N

ALLUVIAL CHANNEL FLOW RESISTANCE: STOCHASTIC PROPERTIES

Project Objective 4

by

(10) Neil L. Coleman 1/  
and  
Robert B. Wilson 2/

USDA Sedimentation Laboratory

Oxford, Mississippi

April 1981

(12/35)

Prepared for

US Army Corps of Engineers, Vicksburg District  
Vicksburg, Mississippi

Under

Section 32 Program, Work Unit 7

1/ Geologist; Research Leader, Sediment Transport and Deposition Research Unit, USDA Sedimentation Laboratory, Oxford, MS.

2/ Computer Specialist, USDA Sedimentation Laboratory, Oxford, MS.

4L6.115

## PREFACE

The work reported here is a part of a general project on alluvial channel flow resistance. The purposes of this project are to study the characteristics of the Darcy-Weisbach resistance coefficient in an alluvial channel under conditions of (a) constant depth and discharge; (b) constant depth and discharge changing with time; (c) constant discharge and depth changing with time. This report covers only condition (a) above.

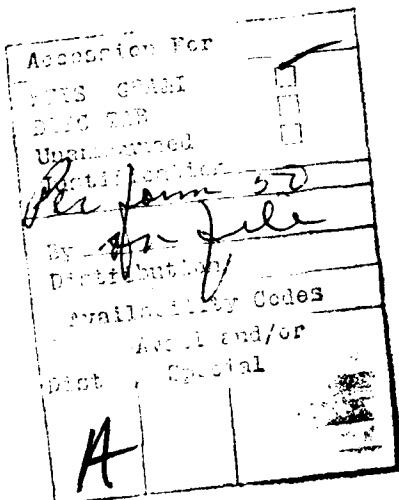


## Table of Contents

LIST OF TABLES

1	Experimental success summary . . . . .	18
2	Summary of time-trend data processing and analysis . . . . .	24

#### LIST OF FIGURES

1	Schematic of the experimental set-up . . . . .	13
2	Cumulative size frequency distribution of the sediment used in the experiments. The y-axis is cumulative percent probability . . . . .	16
3	Typical stationary records of (a) $f$ and (b) $D_s$ . . . . .	22
4	Typical nonstationary records of (a) $f$ and (b) $D_s$ . . . . .	23
5	Resistance functions for subcritical and supercritical flow regimes . . . . .	27
6	Weak correlation between $\sigma_f/\sigma_D$ and $\langle f \rangle$ . . . . .	29
7	The lack of coupling between $I_f$ and $I_D$ . . . . .	30
8	The lack of correlation between $\sigma_f/\langle f \rangle$ and the relative roughness . . . . .	32

**CONVERSION FACTORS, U.S. CUSTOMARY TO METRIC (SI) AND  
METRIC (SI) TO U.S. CUSTOMARY UNITS OF MEASUREMENT<sup>1/</sup>**

**Units of measurement used in this report can be converted as follows:**

To convert	To	Multiply by
mils (mil)	micron ( $\mu\text{m}$ )	25.4
inches (in)	millimeters (mm)	25.4
feet (ft)	meters (m)	0.305
yards (yd)	meters (m)	0.914
miles (miles)	kilometers (km)	1.61
inches per hour (in/hr)	millimeters per hour (mm/hr)	25.4
feet per second (ft/sec)	meters per second (m/sec)	0.305
square inches (sq in)	square millimeters ( $\text{mm}^2$ )	645.
square feet (sq ft)	square meters ( $\text{m}^2$ )	0.093
square yards (sq yd)	square meters ( $\text{m}^2$ )	0.836
square miles (sq miles)	square kilometers ( $\text{km}^2$ )	2.59
acres (acre)	hectares (ha)	0.405
acres (acre)	square meters ( $\text{m}^2$ )	4,050.
cubic inches (cu in)	cubic millimeters ( $\text{mm}^3$ )	16,400.
cubic feet (cu ft)	cubic meters ( $\text{m}^3$ )	0.0283
cubic yards (cu yd)	cubic meters ( $\text{m}^3$ )	0.765
cubic feet per second (cfs)	cubic meters per second (cms)	0.0283
pounds (lb) mass	grams (g)	454.
pounds (lb) mass	kilograms (kg)	0.453
tons (ton) mass	kilograms (kg)	907.
pounds force (lbf)	newtons (N)	4.45
kilogram force (kgf)	newtons (N)	9.81
foot pound force (ft lbf)	joules (J)	1.36
pounds force per square foot (psf)	pascals (Pa)	47.9
pounds force per square inch (psi)	kilopascals (kPa)	6.89
pounds mass per square foot (lb/sq ft)	kilograms per square meter ( $\text{kg}/\text{m}^2$ )	4.88
U.S. gallons (gal)	liters (L)	3.79
quart (qt)	liters (L)	0.946
acre-feet (acre-ft)	cubic meters ( $\text{m}^3$ )	1,230.
degrees (angular)	radians (rad)	0.0175
degrees Fahrenheit (F)	degrees Celsius (C) <sup>2/</sup>	0.555

2/ To obtain Celsius (C) readings from Fahrenheit (F) readings, use the following formula:  $C = 0.555 (F - 32)$ .

Metric (SI) to U.S. Customary

To convert	To	Multiply by
micron ( $\mu\text{m}$ )	mils (mil)	0.0394
millimeters (mm)	inches (in)	0.0394
meters (m)	feet (ft)	3.28
meters (m)	yards (yd)	1.09
kilometers (km)	miles (miles)	0.621
millimeters per hour (mm/hr)	inches per hour (in/hr)	0.0394
meters per second (m/sec)	feet per second (ft/sec)	3.28
square millimeters ( $\text{mm}^2$ )	square inches (sq in)	0.00155
square meters ( $\text{m}^2$ )	square feet (sq ft)	10.8
square meters ( $\text{m}^2$ )	square yards (sq yd)	1.20
square kilometers ( $\text{km}^2$ )	square miles (sq miles)	0.386
hectares (ha)	acres (acre)	2.47
square meters ( $\text{m}^2$ )	acres (acre)	0.000247
cubic millimeters ( $\text{mm}^3$ )	cubic inches (cu in)	0.0000610
cubic meters ( $\text{m}^3$ )	cubic feet (cu ft)	35.3
cubic meters ( $\text{m}^3$ )	cubic yards (cu yd)	1.31
cubic meters per second (cms)	cubic feet per second (cfs)	35.3
grams (g)	pounds (lb) mass	0.00220
kilograms (kg)	pounds (lb) mass	2.20
kilograms (kg)	tons (ton) mass	0.00110
newtons (N)	pounds force (lbf)	0.225
newtons (N)	kilogram force (kgf)	0.102
joules (J)	foot pound force (ft lbf)	0.738
pascals (Pa)	pounds force per square foot (psf)	0.0209
kilopascals (kPa)	pounds force per square inch (psi)	0.145
kilograms per square meter ( $\text{kg}/\text{m}^2$ )	pounds mass per square foot 1b/sq ft)	0.205
liters (L)	U.S. gallons (gal)	0.264
liters (L)	quart (qt)	1.06
cubic meters ( $\text{m}^3$ )	acre-feet (acre-ft)	0.000811
radians (rad)	degrees (angular)	57.3
degrees Celsius (C)	degrees Fahrenheit (F) <sup>3/</sup>	1.8

1/ All conversion factors to three significant digits.

3/ To obtain Fahrenheit (F) readings from Celsius (C) readings, use the following formula:  $F = 1.8C + 32$ .

#### NOTATION

- A Cross sectional area of flow;  
D Water depth;  
 $D_s$  Sand depth;  
 $\langle F \rangle$  Time-mean Froude number;  
 $f$  Instantaneous Darcy-Weisbach coefficient;  
 $\langle f \rangle$  Time-mean Darcy-Weisbach coefficient;  
 $G(t)$  Autocorrelation function;  
g Gravity field strength;  
 $I_D$  Integral time constant of a sand depth record;  
 $I_f$  Integral time constant of a resistance coefficient record;  
 $L_D$  Linear time constant of a sand depth record;  
 $L_f$  Linear time constant of a resistance coefficient record;  
M A coefficient;  
N A constant;  
Q Discharge;  
R Hydraulic radius;  
 $R_e$  Reynolds number;  
r Acceptance region value for runs test;  
 $S_e$  Energy gradient;  
T Water temperature;  
 $T_a$  Total record length of a time-trend record;  
t time;  
U Mean velocity;  
 $U_x$  Shear velocity;  
Z Channel width;  
a Significance level for a runs test;  
 $\sigma_D$  Bedform roughness height;  
 $\sigma_f$  Standard deviation of the instantaneous resistance coefficient;  
v Fluid kinematic viscosity.

## INTRODUCTION

The concept of head loss, energy dissipation, or flow resistance is fundamental to applying physical laws to the design of man-made channels, or to understanding and predicting the behavior of natural channels and rivers. The head loss or resistance concept originated from efforts to understand flow in pipes; its application in this context is so well understood that the design of pipe runs ranging in size from domestic plumbing systems to very large hydraulic power penstocks or oil pipelines has been reduced to a series of fairly standard procedures. The situation is not as well defined with regard to the application of the resistance principle to open channels, where little agreement exists even about how such principles should be applied in the relatively tractable case of channels with rigid linings. In the case of alluvial channels, the situation is so complex that at least one worker (Maddock, 1970) has been led to conclude that alluvial channel flow is hydraulically indeterminate, and that relations between flow depth, velocity, energy gradient, sediment discharge concentration, etc. are artifacts of unrecognized implicit constraints in specific alluvial channel systems, or the results of unrecognized covariances between two or more independent variables. It is certain that every aspect of alluvial channel flow has a stochastic component of relatively large magnitude, and it is undoubtedly this fact that has led to the extreme difficulty experienced by every hydraulician that has ever attempted to understand alluvial channel flow resistance.

This report describes a series of experiments that were performed in a laboratory flume that was adapted to allow computer control of the independent experimental variables, and computer acquisition of data during experiments. The object of the study was to relate the Darcy-Weisbach resistance coefficient of an alluvial channel flow to the bed roughness as expressed by the standard deviation of bed elevation records (a measure of the dune and antidune roughness height). Since the Darcy-Weisbach coefficient in an alluvial channel shows considerable time variation even in supposedly steady uniform flows, and since the bed roughness, as measured from the time records of the bed elevation, is a stochastic quantity; time records of the Darcy-Weisbach coefficient and of the bed elevation were analyzed to obtain probability density functions, which were typified by mean values and standard deviations of the relevant quantities.

Autocorrelation functions of the time records were also computed and plotted. From these functions, time constants for variation of the resistance coefficient and for the propagation of bed forms were obtained.

The Darcy-Weisbach resistance coefficient is of importance in the development of mathematical models of streamflow for predicting floodwave propagation, channel bed and bank modification, and the intensity of fluvial attack on channel protection or river training structures.

## SURVEY OF LITERATURE RELEVANT TO PRESENT STUDY

The Darcy-Weisbach coefficient for an alluvial channel can be defined (Rouse, 1946) as:

$$f = 8U_*^2/U^2 = (8gRS_e)/U^2 \quad (1)$$

where  $U_*$  is the shear velocity at the channel periphery,  $U$  is the mean flow velocity,  $R$  is the hydraulic radius,  $S_e$  is the energy gradient, and  $g$  is gravity field strength. The nature of  $f$  in alluvial channels has been studied by Alam, Cheyer, and Kennedy (1966), who sought a predictor for  $f$  as a function of mean velocity  $U$ , channel hydraulic radius  $R$ , and  $D_{50}$ , which is the median diameter of the sediment comprising the channel bed. At about the same time, Vanoni and Hwang (1967) investigated the relation between the length and height of bed forms and the resistance coefficient. They found a relation involving a bed configuration-area adjusted roughness height which gave a semilogarithmic relative roughness-resistance relation of the same functional form as the Nikuradse (1933) rough pipe formula. This was an important step, since it totally verified the importance of bed forms as roughness elements. However, the results were based on individual determinate measurements of the heights of bed configurations, and it was recognized that some sort of overall effective roughness height that was statistically related to an ensemble of bed forms (a bed configuration) was needed. Nordin and Algert (1966) and Nordin (1971) provided the transition from determinate measurement to stochastic treatment of bed configurations as time-records of bed elevation taken by some sort of sensor as bed forms propagated past a point. Willis (1968) and Willis and Kennedy (1977) postulated that the standard deviation of the time-record of bed elevation at a point might be used as the effective roughness height for a bed configuration, and that this variable, or some function of it, might be substituted for the determinate roughness measure of Vanoni and Hwang. The study reported here tests that hypothesis.

## EXPERIMENTAL EQUIPMENT

The flume used in the experiments reported here was 100 ft. long, 4 ft. wide, and 2 ft. deep. It was originally designed as a conventional variable-slope recirculating flume, and was equipped for manual control of independent variables such as depth and discharge. Data acquisition was also manual. The flume has been adapted for control and data acquisition using a ModComp II computer with 64K words of memory, and capability for analog-to-digital conversion. In addition, this computer was linked during these experiments to the main computer of the Sedimentation Laboratory. This was a ModComp IV multiprogramming computer system with 256K words of memory, bulk disk storage, magnetic tape storage, and data plotting capabilities. It provided extra capability for data analysis.

Fig. 1 is a schematic drawing of the flume as it was arranged for these experiments. At the upstream end of the channel, the first 10 ft. was taken up by an entrance works consisting of vertical flow straightening vanes, a 0.25 ft. sill across the channel just below the vanes, and a tethered raft. These installations contained the most pronounced bed and water surface disturbances due to entrance conditions to a region within the first 30 ft. of channel. Flow cross sections at distances 44.75 and 54.75 ft. down the channel were equipped with flush-mounted pressure transducers in the flume bottom for measuring the sand depth, and special large sidewall fittings connected by flexible tubing to floor-mounted standpipes, located to one side of the channel, and containing capacitance-type wave gauges for measuring the water surface elevation. The use of flush-mounted sand depth sensors and water surface sensors located outside the channel was dictated by the need to keep the instrumentation as noninvasive as possible, to avoid extraneous head losses across the study reach where the resistance coefficient was to be determined. The cross sections containing the equipment discussed above were 10 ft. apart. At points on the flume centerline, 5 ft. above the upstream cross section and 1 ft. below the downstream cross section, total head tubes of small diameter were installed. These total head tubes were connected to a pair of open manometer tubes with a differential pressure transducer between them, to form a differential total head meter of the type used by Gee (1975). The two total head tubes, and the temperature probe shown in Fig. 1, were the only invasive instruments used, and as arranged, they were kept

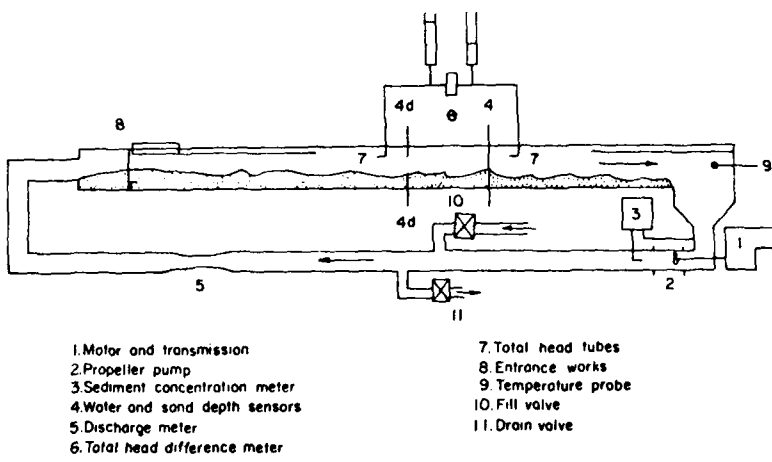


Fig. 1. Schematic of the experimental set-up.

out of the study reach proper. Discharge was monitored by a Venturi meter in the return pipe under the flume, as shown in Fig. 1. A differential pressure transducer was used to measure the pressure drop across the Venturi meter.

All the data acquisition equipment described above transmitted analog voltage signals to the computer, where the analog signals were sampled at a rate of 20,000 samples per second, and digitized. The digital values so obtained were "instantaneous" values with high frequency components greater than or equal to the sampling rate filtered out. In this way transmission line noise and other stray voltages were eliminated, and the significant stochastic variations of the hydraulic variables themselves were retained. McQuivey (1957) found that, in studies of turbulence in water, nearly all the significant spectral components had frequencies less than 100 Hz, with the spectral maxima being in the range of 2 to 8 Hz. Willis and Kennedy (1977) found various spatial and temporal moments of dune and antidune bed configurations to have significant spectral components on the order of 1 Hz or less, so it was reasoned that, in these experiments, the total head difference along the channel test reach, which in rough turbulent flow is highly dependent on bed state, would also be a relatively low-frequency phenomenon.

For setting up the experiments, computer control of water depth was achieved using motor-activated drain and fill valves in the flume return pipe. These values could be activated by the digital output capability of the computer. The water surface elevation sensor at the section labeled 4d in Fig. 1 was given a dual function. In addition to its role as a data collector during an experiment, it acted as a feedback sensor by means of which the computer could compare the actual water surface elevation in the flume with that specified by the operator in initiating an experiment. By repeated comparison and relay operation, the computer could activate the fill and drain valves alternately until the desired water surface elevation was reached. Computer control of discharge was obtained by using the discharge meter as a feedback sensor by means of which the computer could compare the actual discharge with the discharge specified in initiating an experiment. By means of its digital output capability, the computer could operate relays connected in parallel with the manual pushbuttons normally used to adjust the pump speed until the specified discharge was attained.

A cumulative size frequency curve for the sediment used in the experiments is shown in Fig. 2. This material had a median diameter of 0.44 mm.

The sediment concentration meter shown in Fig. 1 was a vertically-mounted vibrating U-tube device similar to that used by Willis and Kennedy (1977). The inlet leg of this meter was connected to a sampling tube located in the flume return pipe just downstream from the pump output, where the sediment was all in suspension and uniformly distributed over the pipe cross section. The outlet leg of the meter was connected to a fitting on the suction side of the pump. With this arrangement, a very nearly isokinetic sampling situation was created, since the speed of flow through the concentration meter was controlled by the speed of the sediment-water mixture coming out of the pump. This concentration meter malfunctioned continually throughout the experimental series, and its concentration measurements, which in any case are of only minor importance in channel resistance studies (Vanoni and Hwang, 1967) will not be discussed here.

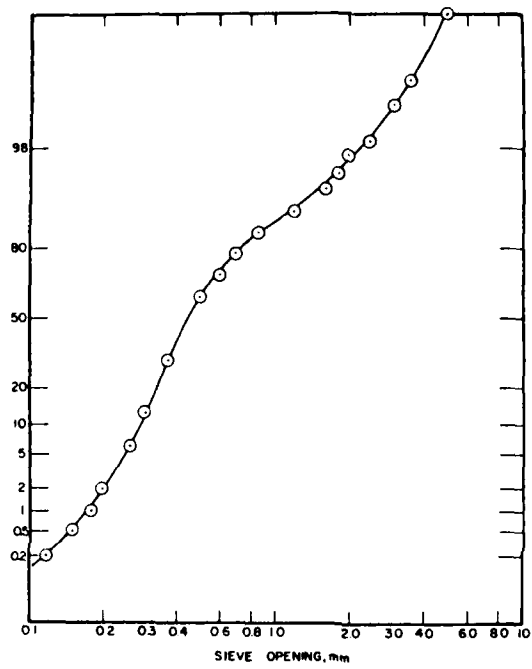


Fig. 2. Cumulative size frequency distribution of the sediment used in the experiments. The y-axis is cumulative percent probability.

## PROCEDURES

In the experimental procedure that was used, the volume of water in the recirculating flume was held constant during an experiment. The discharge was also kept constant by maintaining a constant pump speed. The flume slope was kept at zero, and the sand bed in the flume was allowed to adjust to its natural slope for the depth and discharge conditions imposed. Once this adjustment was complete, a condition existed in which the flow depth, discharge, and energy gradient were all stationary in the sense that their time-mean values were constant over long periods. In this state, the energy gradient across the study reach would display short-term statistical variation that should be related to the nature of the bed state (dunes, antidunes, or whatever) being generated by the flow, and thus, to the flow regime existing.

The experiments were performed with the aid of a computer program that implemented both the initialization, or control, and the data acquisition parts of an experiment. The flume was first manually filled with water to an arbitrary level. After adjusting various gain controls to get all instruments into calibration, and manually starting the pump, appropriate commands were entered into the computer to cause it to adjust the water surface elevation and the discharge to the desired values. When this process was completed, the computer shifted from the initialization mode to the data acquisition mode, and waited for further operator commands.

At the end of the initialization period, the flume was allowed to run long enough for the sand bed to adjust to its natural slope and bed state. For any given experiment, the time required depended on the water depth and discharge, and also on whether the conditions to be imposed were greatly different from those of the preceding experiment. The true data acquisition period began when it was certain that the sand bed had reached its final condition. On operator command, the computer processed the analog outputs of all the instruments, sampling at 20,000 samples per second for 200 samples, and averaging the results. These digitized inputs were then used with the calibration functions of the various instruments to calculate raw data values, which were held in disk storage for further processing and for recording on magnetic tape. The total time needed to read all the instruments and to perform the calculations for each set of digital readings was 0.19 minutes.

Some difficulty was experienced in getting the total head difference meter to function for long periods without having its total head tubes stopped with sediment. After a number of trials, a 50-sample data collection sequence, with a period of 9.67 minutes, was selected as standard for these experiments. It was essential to have a definite predetermined end to the data record because the disk storage capability of the computer required that an endfile mark be inserted at the end of each data set so that it could later be retrieved separately. A typical working day sequence of experiments at a single water level and discharge included five to seven runs, of which one to three would be unacceptable because of instrument stoppages. Table 1 summarizes the degree of success of the experimental sequences reported here. Sequences run for program and instrument testing and development only are not included.

Table 1 shows that, out of a total of 131 runs, 112 were completed acceptably. This illustrates the difficulty of keeping the automated differential total head meter operating. Table 1 also shows the water levels and the average discharges for each sequence of runs.

Table 1. Experimental success summary.

Water level	Average Discharge	Total runs	Acceptable runs
1.50	5.0	7	4
1.50	4.8	4	3
1.50	5.9	8	7
1.50	7.4	5	5
1.50	8.0	7	6
1.50	9.4	5	5
1.49	9.8	6	6
1.52	10.9	5	5
1.49	11.7	7	4
1.50	12.1	3	1
1.00	5.5	7	6
1.01	6.2	5	4
1.00	8.0	7	5
1.05	7.3	5	5
0.98	9.3	5	5
1.26	5.0	6	5
1.26	5.7	5	5
1.24	7.5	5	5
1.28	8.5	6	5
1.24	9.1	5	5
1.24	10.0	6	5
1.24	10.9	5	5
1.26	12.5	7	6

## INITIAL DATA PROCESSING AND ANALYSIS

The raw data from each experiment that was held in disk storage consisted of instantaneous values of time, discharge, water depth and sand depth at each end of the study reach, energy gradient across the study reach, and water temperature. After each set of experiments, another computer program used this raw data to calculate needed derived variables. The areas  $A_1$  and  $A_2$  at the upstream and downstream ends of the study reach, respectively, were calculated from:

$$A_i = D_i Z \quad i = 1, 2 \quad (2)$$

where  $D$  is the water depth and  $Z$  is the flume width. The mean velocities at each end of the reach were computed from:

$$V_i = Q/A_i \quad i = 1, 2 \quad (3)$$

where  $Q$  is the discharge. The hydraulic radius at each end of the reach was calculated from:

$$R_i = A_i / (Z + 2D_i) \quad i = 1, 2 \quad (4)$$

Then the spatially averaged hydraulic radius and the spatially averaged mean velocity for the reach were found from:

$$R = (R_1 + R_2)/2 \quad (5)$$

and

$$V = (V_1 + V_2)/2 \quad (6)$$

The representative reach Reynolds number was calculated from:

$$R_e = 4RU/v \quad (7)$$

where  $v$  is the kinematic water viscosity calculated using water temperature values,  $T$ , and the equation:

$$v = 3.42 - (6.17 \times 10^{-2})T + (5.14 \times 10^{-4})T^2 - (2.28 \times 10^{-6})T^3 + (3.68 \times 10^{-9})T^4 \quad (8)$$

This viscosity relation was obtained by fitting a polynomial to a table of viscosity values at different water temperatures that was given by Rouse (1946). The representative instantaneous Darcy-Weisbach resistance coefficient for the reach was calculated from:

$$f = 8U_*^2/U^2 = 8gRS_e/U^2 \quad (9)$$

using  $R$  and  $U$  from equations (5) and (6), and where  $g$  is gravity field strength and  $S_e$  is the energy gradient from values stored in the raw data.

Both the raw data and the derived data were stored on magnetic tape at the end of each sequence of experiments, so as to be available for time record analysis.

## TIME RECORD ANALYSIS AND RESULTS

The principle aim of this research was to relate stochastic properties of  $f$  to stochastic properties of bed configurations on the alluvial channel bed. For this purpose, time records of instantaneous values of the resistance coefficient  $f$  were subjected to runs tests (Bendat and Piersol, 1966) for stationarity of record, and to autocorrelation analysis to determine the integral time scale of the record. By-products of this second analysis were the time-mean value  $\langle f \rangle$  of the resistance coefficient, and the standard deviation  $\sigma_f$  of the instantaneous resistance coefficients in the record.

The testing of each record for its stationarity was believed advisable because of the short record period that was imposed on the experiments by the propensity of the total differential head meter to malfunction. It was thought that this might result in some highly nonstationary records, and that data from these records might differ significantly from that included in stationary records. The integral time scale of  $f$  is a measure of the mean period of fluctuation. The time-mean value  $\langle f \rangle$  is the steady-state value of  $f$ , while the standard deviation,  $\sigma_f$ , of  $f$ , is a measure of the intensity of variation, particularly when combined into the coefficient of variation  $\sigma_f/\langle f \rangle$ .

The same two analyses were performed on the records of sand depth (more properly, sand bed surface elevation) as measured by the sand depth sensor at the upstream end of the study reach. Again, it was believed advisable to test the records for stationarity, particularly since it was intended that  $\sigma_D$ , the standard deviation of the bed elevation from a single record, was to be used as a representative measure of the effective roughness height of the bed configuration existing when that record was taken. The integral time scale of the sand depth record may be interpreted as the mean time taken for bed forms propagating on an alluvial bed to pass a given point, and thus it is a feasible method of inferring bed configuration length when temporal, and not spatial, records are available. In the context of the experiments done here, the time-mean sand depth has no significance; however, as suggested by Willis and Kennedy (1977) the standard deviation  $\sigma_D$  of the sand depth may be a significant measure of the roughness height of bed configurations.

Mathematical definitions of the runs tests and autocorrelation analyses used are given below.

Table 2 is a summary of the data analysis results. Included are the time-mean resistance coefficient,  $\langle f \rangle$ ; the standard deviation,  $\sigma_f$ , of the resistance coefficient; and the integral time constant,  $I_f$ , of the resistance coefficient. The standard deviation,  $\sigma_D$ , of the sand depth, and the sand depth integral time constant,  $I_D$ , are also included. As an index of gross flow conditions, both the time-mean Reynolds number,  $\langle R_e \rangle$ , and the time-mean Froude number:

$$\langle F \rangle = \langle U / (gR) \rangle^{1/2} \quad (10)$$

are given in the table.

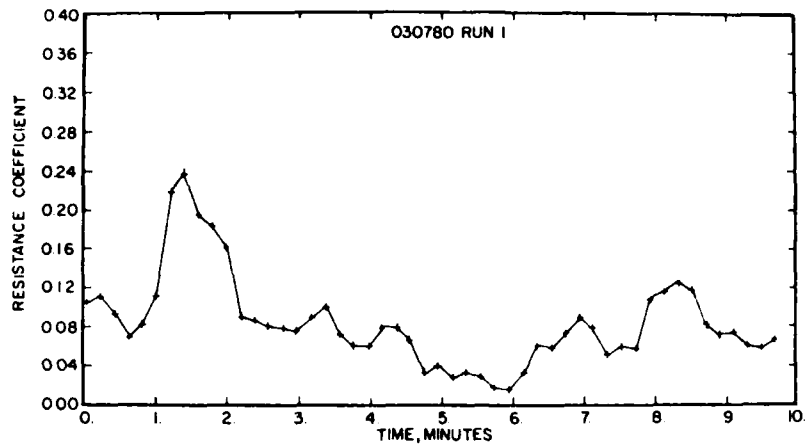
The runs test for stationarity of record that was applied was a test described by Bendat and Piersol (1966). In this test, the median value of a time record of data is taken as a standard. Then runs of individual data values above and below the median are counted. The number of runs is  $r$ , and the acceptance region for the test is  $r_{y;1-\alpha/2} \leq r \leq r_{y;\alpha/2}$ , where  $y$  was 25 because there were 50 data values in each record. The acceptance level  $\alpha$  was taken as 0.05, and the region,  $r_{25;0.975} \leq r \leq r_{25;0.025}$ , equal to 18  $\leq r \leq 33$  was found from a table of percentage points for runs distributions given by Bendat and Piersol.

The results of the runs tests for stationarity of record are shown in Table 2 by asterisks that indicate which values of  $\langle f \rangle$  and  $\sigma_D$  were calculated from stationary records. Figures 3a and 3b are, respectively, typical stationary records of  $f$  and  $D_s$ , while Figs. 4a and 4b are typical nonstationary records. Out of the 112 experimental runs in Table 2, only 39 displayed stationary records of  $f$  and  $\sigma_D$  simultaneously. This is almost certainly a result of the short record length imposed on the experiments by the probability of instrument stoppages.

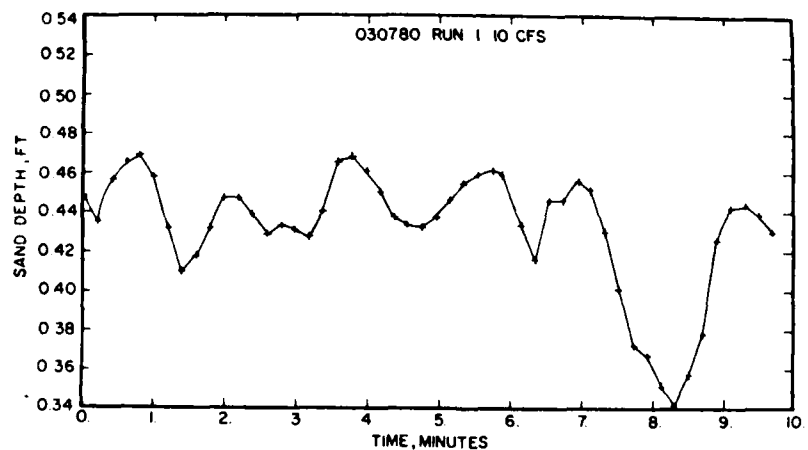
The integral time constants  $I_f$  and  $I_D$  given in Table 2 were found in two steps. The first step was computation of the autocorrelation function

$$G_a(t^*) = [\sum(a')_{t^*} (a')_{t^*+\Delta t^*}] / \sum(a')^2 \quad (11)$$

where  $a$  is either  $f$  or  $D_s$ , and  $a'$  is the deviation of either variable from its mean, while  $t^*$  is time normalized by the total record time  $T_a$ . The second step was integration under the autocorrelation function to obtain

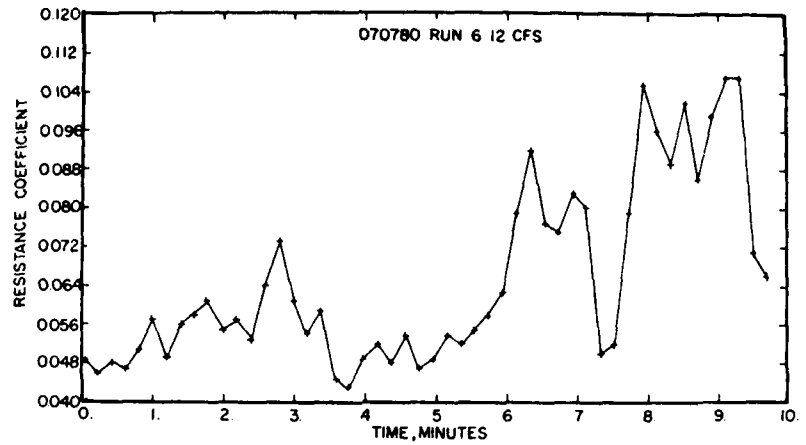


(a)

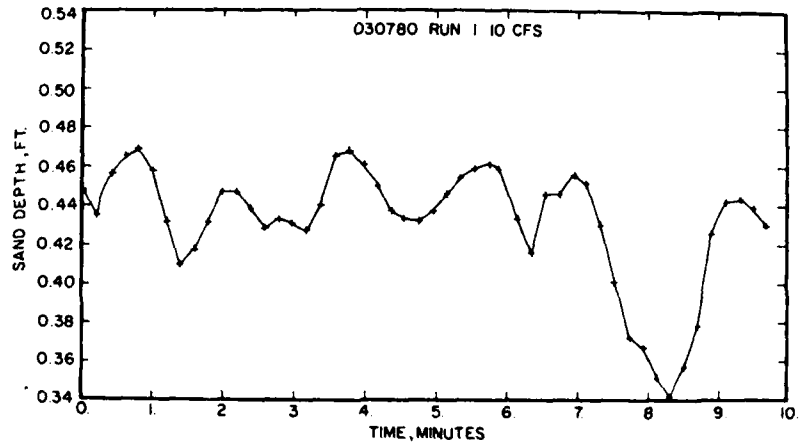


(b)

Fig. 3. Typical stationary records of (a)  $f$  and (b)  $D_s$ .



(a)



(b)

Fig. 4. Typical nonstationary records of (a)  $f$  and (b)  $D_s$ .

Table 2. - Summary of time-trend data processing and analysis.

$\langle R_e \rangle$ $\times 10^{-5}$	$\langle F \rangle$	$\langle f \rangle$	$\sigma_f$	$I_f$	$\sigma_D$	$I_D$
3.57	0.25	0.116*	0.047	0.045	0.001	0.098
3.68	0.27	0.099*	0.031	0.045	0.002	0.135
3.63	0.26	0.059*	0.022	0.041	0.003	0.166
3.76	0.29	0.070*	0.020	0.012	0.001*	0.039
3.47	0.26	0.069*	0.023	0.093	0.001*	0.046
3.47	0.26	0.052*	0.023	0.017	0.001	0.098
3.46	0.26	0.060*	0.023	0.038	0.001*	0.014
4.28	0.32	0.092*	0.030	0.026	0.002	0.131
4.25	0.32	0.068	0.026	0.080	0.003	0.181
4.28	0.32	0.053*	0.022	0.058	0.002	0.162
4.32	0.32	0.047	0.015	0.017	0.010	0.180
4.32	0.33	0.108	0.019	0.030	0.006	0.112
4.34	0.33	0.138	0.063	0.090	0.007	0.152
4.32	0.33	0.100	0.024	0.076	0.006	0.130
5.36	0.35	0.127*	0.043	0.013	0.034	0.115
5.20	0.36	0.104*	0.043	0.014	0.013	0.160
5.17	0.36	0.081*	0.029	0.029	0.025*	0.011
5.54	0.22	0.052*	0.020	0.052	0.025	0.176
5.41	0.38	0.058*	0.019	0.043	0.057	0.179
5.62	0.40	0.206*	0.029	0.018	0.042	0.184
5.61	0.40	0.134*	0.038	0.050	0.021	0.152
5.64	0.38	0.141	0.035	0.086	0.032	0.185
5.68	0.40	0.127	0.065	0.169	0.011*	0.108
5.68	0.38	0.090	0.049	0.090	0.062	0.154
5.56	0.36	0.100*	0.035	0.012	0.015*	0.134
6.58	0.45	0.097*	0.033	0.024	0.007	0.153
6.26	0.37	0.278*	0.105	0.095	0.081	0.053
6.62	0.44	0.112*	0.038	0.074	0.070	0.144
6.51	0.42	0.136*	0.049	0.063	0.019	0.168
6.55	0.42	0.143*	0.045	0.020	0.064*	0.170
6.82	0.50	0.074*	0.022	0.013	0.024*	0.058
7.00	0.53	0.080*	0.025	0.094	0.011	0.156
7.18	0.54	0.042*	0.015	0.024	0.071	0.183
6.89	0.47	0.113*	0.034	0.076	0.057	0.138
6.98	0.52	0.086*	0.036	0.054	0.010	0.164
6.78	0.48	0.111	0.068	0.079	0.046	0.106
8.07	0.64	0.066	0.027	0.124	0.073	0.166
7.95	0.60	0.074*	0.025	0.052	0.056	0.179
8.14	0.67	0.029*	0.013	0.031	0.041	0.183
7.76	0.56	0.107*	0.058	0.059	0.103*	0.126
7.92	0.57	0.072*	0.021	0.024	0.114	0.150
8.46	0.60	0.073*	0.038	0.049	0.090*	0.159
8.54	0.58	0.104*	0.031	0.021	0.080*	0.132
8.82	0.64	0.069*	0.022	0.038	0.107*	0.145
8.74	0.62	0.040	0.029	0.061	0.039	0.142
8.26	0.54	0.117*	0.038	0.076	0.121	0.169
4.88	0.84	0.059*	0.018	0.024	0.022*	0.076

Table 2. (Cont'd)

4.93	0.77	0.061*	0.024	0.069	0.043*	0.096
4.84	0.79	0.103*	0.058	0.151	0.032*	0.094
4.86	0.82	0.050*	0.033	0.078	0.011*	0.066
4.96	0.80	0.044	0.023	0.062	0.021	0.067
5.44	0.74	0.115*	0.080	0.075	0.019*	0.073
5.61	0.79	0.072*	0.024	0.113	0.054*	0.096
5.32	0.70	0.107	0.051	0.094	0.036	0.061
5.46	0.78	0.060*	0.037	0.079	0.048*	0.102
5.42	0.76	0.104*	0.037	0.052	0.041*	0.126
7.01	0.92	0.078*	0.028	0.036	0.016	0.027
6.92	0.88	0.052*	0.014	0.035	0.031	0.100
6.64	0.67	0.083	0.040	0.068	0.045	0.063
7.10	0.91	0.077*	0.023	0.024	0.033	0.071
7.13	0.87	0.072*	0.025	0.035	0.020*	0.039
6.10	0.58	0.135	0.052	0.055	0.051*	0.102
6.13	0.66	0.120	0.054	0.116	0.043*	0.047
6.54	0.21	0.126	0.063	0.117	0.032*	0.096
6.51	0.22	0.108*	0.057	0.078	0.028*	0.044
6.58	0.22	0.103*	0.029	0.045	0.051*	0.111
8.24	1.52	0.025*	0.003	0.013	0.009*	0.078
8.28	1.51	0.023*	0.005	0.014	0.006*	0.015
8.38	1.49	0.023*	0.004	0.046	0.015*	0.088
8.34	1.49	0.023*	0.005	0.044	0.013*	0.101
8.42	1.49	0.023*	0.006	0.070	0.023*	0.130
3.96	0.42	0.112*	0.043	0.059	0.021	0.125
4.00	0.43	0.124	0.028	0.044	0.011	0.178
3.86	0.38	0.177*	0.035	0.014	0.030	0.176
3.91	0.40	0.157*	0.031	0.026	0.013*	0.138
3.93	0.41	0.092*	0.027	0.038	0.006	0.164
3.88	0.34	0.096	0.033	0.095	0.032*	0.117
4.56	0.42	0.117	0.050	0.080	0.052	0.159
4.42	0.39	0.168*	0.029	0.576	0.027*	0.113
4.49	0.41	0.166*	0.027	0.059	0.010	0.154
4.46	0.40	0.164*	0.038	0.196	0.048	0.171
4.56	0.43	0.091*	0.034	0.046	0.009	0.126
6.07	0.70	0.128*	0.016	0.041	0.060*	0.118
6.22	0.78	0.047*	0.014	0.041	0.015	0.136
6.21	0.67	0.065*	0.014	0.050	0.065	0.181
6.22	0.74	0.031	0.019	0.118	0.022	0.066
5.96	0.60	0.061*	0.033	0.066	0.038*	0.126
6.91	0.66	0.068	0.020	0.071	0.063*	0.100
6.70	0.60	0.164	0.060	0.152	0.038*	0.072
6.98	0.69	0.048*	0.026	0.038	0.028	0.056
7.02	0.63	0.081*	0.044	0.065	0.118	0.154
7.07	0.76	0.117*	0.039	0.068	0.040	0.074
7.41	0.68	0.112	0.035	0.003	0.030	0.168
7.51	0.73	0.106*	0.038	0.004	0.050	0.086
7.61	0.71	0.085*	0.088	0.009	0.103*	0.136
7.39	0.66	0.045*	0.018	0.002	0.039*	0.073
7.34	0.63	0.117	0.034	0.004	0.035	0.095
8.44	0.78	0.084*	0.047	0.005	0.030*	0.051

8.37	0.76	0.055*	0.024	0.002	0.020*	0.058
8.04	0.63	0.094*	0.026	0.002	0.047*	0.121
7.96	0.58	0.119	0.052	0.005	0.088*	0.162
8.11	0.64	0.077	0.031	0.003	0.046	0.083
9.63	1.01	0.037*	0.020	0.002	0.019*	0.076
9.06	0.84	0.062	0.034	0.004	0.070*	0.092
9.62	0.96	0.058*	0.017	0.002	0.034*	0.069
9.63	1.01	0.052	0.008	0.001	0.010*	0.025
10.38	0.89	0.060*	0.025	0.002	0.030	0.102
10.33	0.86	0.097*	0.026	0.002	0.042	0.155
10.09	0.73	0.102*	0.057	0.006	0.039*	0.065
10.74	0.96	0.066*	0.022	0.002	0.014	0.028
10.68	0.96	0.065	0.019	0.002	0.019	0.082
10.61	0.94	0.065*	0.018	0.002	0.015*	0.032

\*Values calculated from stationary records.

$$I_a = \int_0^{L_a^*} G_a(t^*) dt^* \quad (12)$$

where  $L_a^*$  is the normalized time to the first zero crossing ( $t^* = L_a^*$ ,  $G_a(t^*) = 0$ ). The integral time constants for  $f$  and  $D_s$  found in this way are nondimensional.

Vanoni and Hwang (1967) found it necessary to introduce a weighting factor, consisting of the ratio between the projected horizontal area of lee dune and ripple faces to the total horizontal area of the study reach bed, in order to use the deterministically measured dune or ripple height as the roughness height in a classical resistance formula of the Nikuradse (1933) type. By analogy, in using the statistical measure  $\sigma_D$  as a roughness height, a weighting factor must be introduced. This factor is the nondimensional time constant  $I_D$ . The relative roughness of the channel is then  $(4R I_D / \sigma_D)$ . In the classical Nikuradse form, a resistance function for fully rough turbulent flow should be:

$$1/\langle f \rangle^{\frac{1}{2}} = M \log(4R I_D / \sigma_D) + N \quad (13)$$

where  $M$  is a coefficient and  $N$  is a constant.

In Fig. 5 the resistance data are plotted in the coordinates of eq. (13). Although considerable scatter exists, the data clearly define two

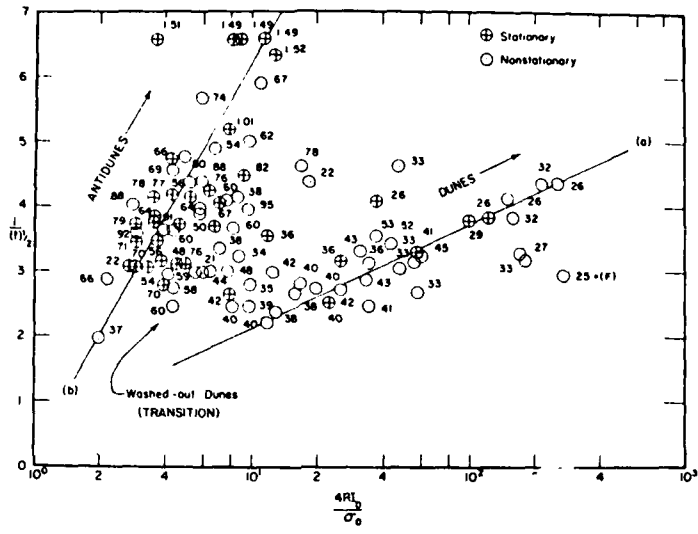


Fig. 5 Resistance functions for subcritical and super critical flow regimes.

functions, with a transition between them. These functions may be classified respectively as a low Froude number function and a high Froude number function, with the transition taking place over the range  $0.4 < F < 0.7$ . The sequence of events portrayed in Fig. 5 was visually confirmed during the experiments. Beginning with the most tranquil flows ( $F \approx 0.2$ ) dunes were observed. These dunes became longer relative to their height as  $F$  increased, and were gradually eliminated in favor of antidunes by a washing-out process. It is significant that the greatest energy dissipation (Minimum values of  $1/\langle f \rangle^{\frac{1}{2}}$ ) is displayed just at the beginning of transition. Beyond this particular flow regime, energy dissipation rapidly decreases (high values of  $1/\langle f \rangle^{\frac{1}{2}}$ ) as the large separation zones behind the dunes are eliminated. The limiting resistance functions for the low and high Froude number cases respectively can be tentatively defined from the data as:

$$1/\langle f \rangle^{\frac{1}{2}} = 1.6 \log (4RI_D/\sigma_D) + 0.5 \quad (14)$$

and

$$1/\langle f \rangle^{\frac{1}{2}} = 4.2 \log (4RI_D/\sigma_D) + 0.2 \quad (15)$$

In Fig. 5 the data points representing experiments in which the records of  $f$  and  $\sigma_D$  were simultaneously stationary have been distinguished from the others by special symbols, as shown in the legend. Since there does not seem to be any difference between the trends displayed by the stationary and the nonstationary data points, all the data has been used in defining eqs. (14) and (15).

Willis and Kennedy (1977) have shown that the various statistical parameters of bed configurations are governed by the bed states which appear under different subcritical and supercritical flow regimes. Therefore, it would be expected that relations between  $\sigma_f$  and  $\sigma_D$  and between  $I_f$  and  $I_D$  would exist, and that the nature of these relations would be governed by the Froude number. To test this, the ratios  $\sigma_f/\sigma_D$  and  $I_f/I_D$  were plotted against  $F$  in Figs. 6 and 7, respectively. There is only the most tenuous hint of a correlation in Fig. 6, indicating that if a relation between  $\sigma_f$  and  $\sigma_D$  exists, its form will indeed be governed by the Froude number, but that the relation cannot be found, even tentatively, from these data. In Fig. 7 no correlation whatever is evident, demonstrating the lack of coupling between  $I_f$  and  $I_D$ . Plots of  $\sigma_f/\sigma_D$  were also made against the

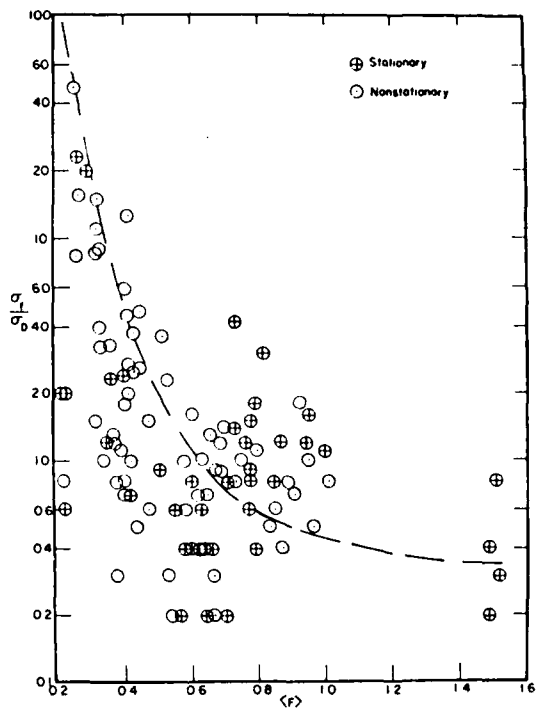


Fig. 6 Weak correlation between  $\sigma_f/\sigma_D$  and  $\langle F \rangle$ .

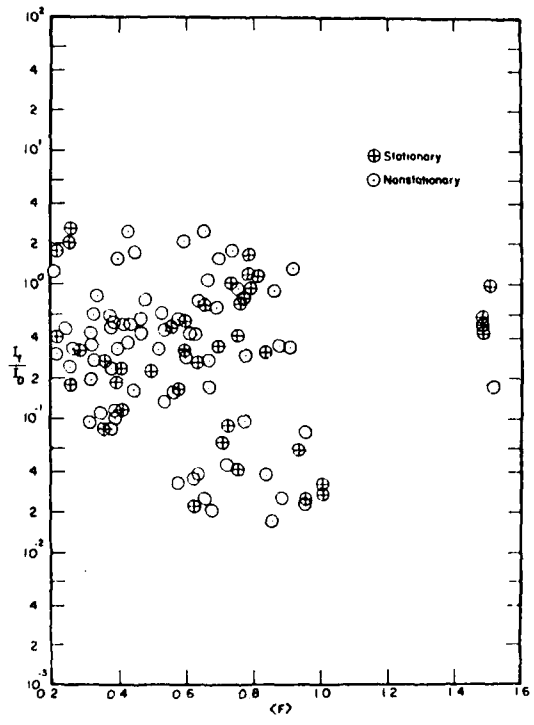


Fig. 7 The lack of coupling between  $I_f$  and  $I_D$ .

Reynolds number, with inconclusive results similar to those shown in Figs. 6 and 7. These plots are not included here, as they contain no information.

The relative statistical variation of  $f$  is expressed by the coefficient of variation,  $\sigma_f/\langle f \rangle$ . Since the weighted relative roughness has proven to be the appropriate variable for correlating  $1/\langle f \rangle^{\frac{1}{2}}$ , it was also tested as the correlating parameter for  $\sigma_f/\langle f \rangle$ , as in Fig. 8. No correlation was found. Evidently the temporal variation of  $f$  around a particular value of  $\langle f \rangle$  is a random phenomenon.

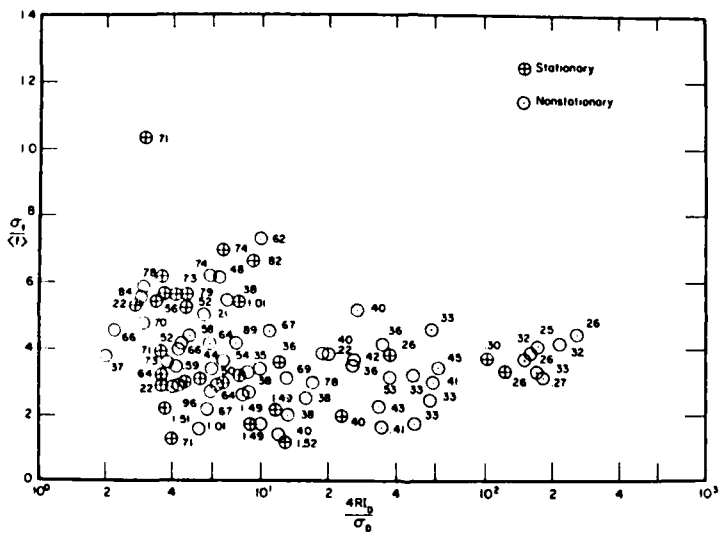


Fig. 8 The lack of correlation between  $\sigma_f/\langle f \rangle$  and the relative roughness.

## CONCLUSIONS

1. A total of 112 experiments were completed in this study without stoppages due to instrument failure. Of these experiments, 39 displayed simultaneous stationary records of the resistance coefficient and the bedform roughness  $\sigma_D$ .
2. Although data scatter was large, tentative time-mean resistance functions could be defined for the subcritical and supercritical flow regimes. These functions were of the Nikuradse (1933) form, in which an expression for relative roughness was the independent variable.
3. The ratio  $(4R/\sigma_D)$  was found to be a usable expression for bedform relative roughness if it was weighted by the nondimensional integral time constant  $I_D$  of sand bed fluctuation to form the relative roughness ratio  $(4RI_D/\sigma_D)$ .
4. For individual time records, only a hint of a relation between  $\sigma_f$  and  $\sigma_D$  was found. If this relation indeed exists, its form will depend on the Froude number.
5. No evidence of coupling could be found between  $I_f$  and  $I_D$ , which are, respectively, the integral time constants of the resistance coefficient of the study reach, and the propagation of bedforms down the study reach.
6. The temporal variation of instantaneous values of  $f$  around the mean value  $\langle f \rangle$  was found to be not related to the relative roughness of the study reach in a given flow.

## REFERENCES

- Alam, A. M. Z., Cheyer, T. F., and Kennedy, J. F., (1966) Friction Factors for Flow in Sand Bed Channels. Mass. Institute of Technology, Dept. of Civil Engineering, Hydraulics Laboratory Report No. 78, 97 pp.
- Bendat, J. S., and Piersol, A. G., (1966) Measurement and Analysis of Random Data. New York:John Wiley and Sons, Inc., 390 pp.
- Gee, D. M., (1975) Bed Form Response to Unsteady Flows. Journal of the Hydraulics Div., ASCE, Vol. 101, HY3, pp. 437-449.
- Maddock, T., Jr., (1970) Indeterminate Hydraulics of Alluvial Channels. Journal of the Hydraulics Div., ASCE, Vol. 96, HY11, pp. 2309-2323.
- McQuivey, R. S., (1967) Turbulence in a Hydrodynamically Rough and Smooth Open Channel Flow. Ph.D. Dissertation, Colorado State University; U.S.G.S. Open-file Report, Oct. 1967, 105 pp.
- Nikuradse, J., (1933) Laws of Flow in Rough Pipes. National Advisory Committee for Aeronautics. Technical Memorandum 1292, 62 pp.
- Nordin, C. F., Jr., and Algert, J. H., (1966) Spectral Analysis of Sand Waves. Journal of the Hydraulics Div., ASCE, Vol. 92, HY 5, pp. 95-114.
- Nordin, C. F., Jr., (1971) Statistical Properties of Dune Profiles. U.S.G.S. Professional Paper 562-F, Washington:U.S.Govt. Printing Office, 41 pp.
- Rouse, H., (1946) Elementary Mechanics of Fluids. New York:John Wiley and Sons, Inc., 375 pp.
- Vanoni, V. A., and Hwang, Li-San, (1967) Relation Between Bed Forms and Friction in Streams. Journal of the Hydraulics Div., ASCE, Vol. 93, No. HY3, pp. 121-144.
- Willis, J. C., (1968) A Lag-deviation Method for Analyzing Channel Bed Forms. Water Resources Research, Vol. 4, No. 6, pp. 1329-1334.
- Willis, J. C., and Kennedy, J. F., (1977) Sediment Discharge of Alluvial Streams Calculated from Bed-form Statistics. State University of Iowa, Iowa Institute of Hydraulic Research, Report No. 202, 199 pp.